

# BZ-MC-BP Model for Jet Production from Black Hole Accretion Disc

Ding-Xiong Wang\*, Yong-Chun Ye, Yang Li and Zhao-Jiang Ge

*Department of Physics, Huazhong University of Science and Technology, Wuhan, 430074, China*

\* Send offprint requests to: D.-X. Wang (dxwang@hust.edu.cn)

30 October 2018

## ABSTRACT

Three energy mechanisms invoking large-scale magnetic fields are incorporated in a model to interpret jet production in black hole (BH) systems, i.e., the Blandford-Znajek (BZ), the magnetic coupling (MC) and Blandford-Payne (BP) processes. These energy mechanisms can coexist in BH accretion disc based on the magnetic field configurations constrained by the screw instability, provided that the BH spin and the power-law index indicating the variation of the magnetic field at an accretion disc are greater than some critical values. In this model the jets are driven by the BZ process in the Poynting flux regime and by the BP process in the hydromagnetic regime, being consistent with the spine/sheath jet structure observed in BH sources of stellar and supermassive size.

**Key words:** accretion, accretion discs — black hole physics — magnetic field — jet production

## 1 INTRODUCTION

As is well known, jets exist in many astronomical cases, such as active galactic nuclei, quasars and young stellar objects. Different theoretical models have been proposed for acceleration and collimation of jets, which can be divided into two main regimes. Energy and angular momentum are carried by both the electromagnetic field and the kinetic flux of matter in the hydromagnetic regime, and those are carried predominantly by the electromagnetic field in the Poynting flux regime (Ustyugova et al. 2000; Lovelace et al. 2002). Blandford & Znajek (1977) proposed firstly that jets from AGNs can be powered by a rotating black hole (BH) with a large scale magnetic field threading its horizon. Later, Blandford & Payne (1982, hereafter BP82) suggested that an outflow of matter can be driven centrifugally by large-scale magnetic fields anchored at the disc surface. These two mechanisms are usually referred to the BZ and BP processes, respectively. As argued in BP82, an outflow of matter can be driven centrifugally from the disc, provided that the angle of the poloidal magnetic field with the normal of disc surface is greater than a critical value, i.e.,  $\alpha_{FL} > 30^\circ$ . The BZ and BP processes belong to the Poynting flux and hydromagnetic regimes, respectively.

Recently, much attention has been paid to the magnetic coupling (MC) of a rotating BH with its surrounding accretion disc, and this mechanism is referred to as the MC process, which can be regarded as a variant of the BZ process (Blandford 1999; Li 2000, 2002a; Wang, Xiao & Lei

2002, Wang et al. 2003, hereafter W02, W03; Uzdensky 2004, 2005). In the MC process energy and angular momentum are transferred from a rotating BH to its surrounding disc. Although the MC process cannot power jet/outflow directly, it plays an important role in depressing disc accretion due to transfer of angular momentum from a rotating BH to the inner disc.

In this paper we incorporate the BZ, MC and BP processes into a model to explain the jets from AGNs and the BH binaries. Henceforth this model is referred to as the BZ-MC-BP model. It turns out that the three mechanisms can coexist, provided that the BH spin and the power-law index indicating the variation of the magnetic field with the disc radius are greater than some critical values. Since the jets could be driven in two regimes (the BZ process in the Poynting flux regime and the BP process in the hydromagnetic regime), this model could be applicable to a spine/sheath jet structure observed in BH sources of stellar and supermassive size (Meier 2003). This paper is organized as follows. In Sect. 2 the magnetic field configuration of the BZ-MC-BP model is outlined. The magnetic field configuration is given based on the constraint of the screw instability, which consists of three parts: region I, II and III corresponding to the BZ, BP and MC processes, respectively. In Sect. 3 the condition for a centrifugally driven outflow of matter from the disc is discussed in a parameter space. The matter outflow rate is determined based on the radial variation of the accretion rate due to the MC effect, and the BP power is derived

based on the work done by the magnetic torque given in BP82. It is shown that the outer boundary radius of region II for the BP process is intimately related to the power-law index indicating the variation of the accretion rate in region III. In Sect. 4 we compare the relative importance of the BZ and BP processes in jet production, and estimate the jet powers as the sum of the BP and the BZ powers. Finally, in Sect. 5, we discuss the potential application of the BZ-MC-BP model to astrophysics. It turns out that the main features of this model are consistent with the general relativistic MHD simulations of accretion and outflow in BH systems.

Throughout this paper the geometric units  $G = c = 1$  are used.

## 2 MAGNETIC FIELD CONFIGURATION OF BZ-MC-BP MODEL

In order to discuss the magnetic extraction of energy and angular momentum from BH accretion disc by virtue of the BZ, MC and BP mechanisms, we must determine the corresponding magnetic field configurations. The difficulty related to this issue lies in two aspects. First, we have not enough knowledge about the origin of magnetic field in the BH accretion disc. Some authors argued that magnetic field could be amplified by virtue of dynamo process at accretion disc, and the magnetic field at the BH horizon is brought from disc accretion and kept by the magnetic pressure of the surrounding disc (MacDonald & Thorne 1982; Ghosh & Abramowicz 1997; Balbus & Hawley 1998). Li (2002b) and Wang et al. (2007) discussed the origin of the magnetic field configuration corresponding to the MC process by assuming a toroidal electric current flowing in the equatorial plane of a Kerr BH. Unfortunately, a reliable origin of large-scale magnetic fields in BH accretion discs remains unclear. Second, we cannot determine the connection between the magnetic field configurations corresponding to the BZ, MC and BP mechanisms.

Lovelace, Romanova & Bisnovatyi-Kogan (1995, hereafter L95) investigated disc accretion of matter on to a rotating star with an aligned dipole magnetic field, and they argued that when the angular velocities of the star and disc differ substantially, the magnetic field linking the star and disc rapidly inflates to give regions of open field lines extending from the polar caps of the star and from the disc. The open field line region of the disc leads to the possibility of magnetically driven outflows.

Wang, Lei & Ye (2006, hereafter W06) proposed a model to explain the light curves of gamma-ray bursts by considering the effects of screw instability of magnetic field. It turns out that the screw instability in the BZ process (henceforth SIBZ) can coexist with the screw instability in the MC process (henceforth SIMC), provided that three parameters are greater than some critical values. These parameters are (i) the BH spin defined as  $a_* \equiv J/M^2$ , (ii) the power-law index  $n$  indicating the variation of the poloidal magnetic field at the disc,  $B_d^p \propto r_d^{-n}$  and (iii) the critical height of the astrophysical load  $H_c$  above the disc surface. The involved quantities  $M$ ,  $J$ ,  $r_d$  and  $B_d^p$  are the BH mass, the BH angular momentum, the disc radius and the poloidal magnetic field at the disc, respectively.

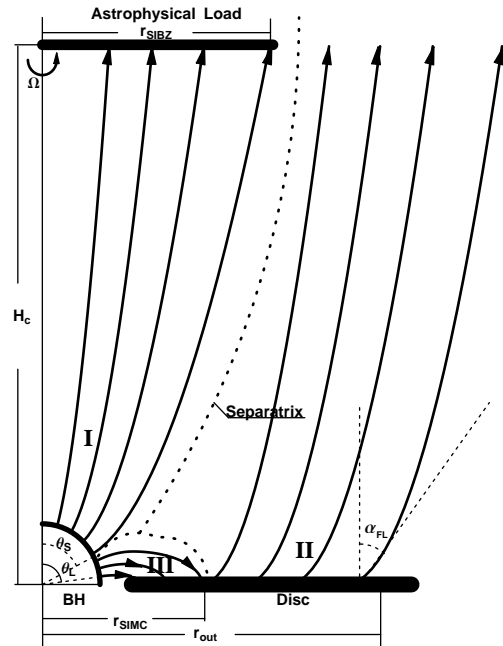


**Figure 1.** Schematic drawing of the magnetic field configuration of the BZ-MC-BP model

In this paper we combine the BZ, MC and BP processes into a model by virtue of the screw instability of the magnetic field. Based on the constraints due to SIMC and SIBZ given in W06 we have the magnetic field configuration related to the BZ-MC-BP model as shown in Figure 1.

In Figure 1  $r_{SIMC}$  is the critical radius constrained by SIMC, which is determined by

$$(2\pi r_{SIMC}/L_{MC}) B_d^p/B_d^T = 1. \quad (1)$$

Similarly,  $r_{SIBZ}$  is the critical radius constrained by SIBZ, which is determined by

$$(2\pi r_{SIBZ}/L_{BZ}) B_L^p/B_L^T = 1. \quad (2)$$

Equations (1) and (2) are derived based on the Kruskal-Shafranov criterion: the screw instability will occur, if the magnetic field line turns around itself about once (Kadomtsev 1966; Bateman 1978). In equation (1)  $L_{MC}$  is the critical length of the poloidal field line for SIMC, and  $B_d^p$  and  $B_d^T$  are the poloidal and toroidal components of the magnetic field on the disc, respectively. In equation (2)  $L_{BZ}$  is the critical length of the poloidal field line for SIBZ, and  $B_L^p$  and  $B_L^T$  are the poloidal and toroidal components of the magnetic field on the astrophysical load, respectively.

As shown in Figure 1, the regions of open field lines at the horizon and disc are referred to as regions I and II, which correspond to the BZ and BP processes, respectively. The region of closed field lines connecting the BH with the disc is referred to as regions III, which corresponds to the MC process. Region I is confined to the angular region at the horizon,  $0 < \theta < \theta_S$ , while region II is confined to the radial region at the disc,  $r_{SIMC} < r < r_{out}$ . Region III is confined to  $\theta_S < \theta < \theta_L$  at the horizon and to  $r_{ms} < r < r_{SIMC}$  at the disc. The angle  $\theta_S$  is the angular boundary between the open and closed field lines on the horizon, and  $\theta_L$  is the

lower boundary angle for the closed field lines. Throughout this paper  $\theta_L = 0.45\pi$  is taken in calculations.

From Figure 1 we find that the magnetic field configuration for the BZ-MC-BP model looks similar to that of L95 (see Figure 3 given in L95). In both cases the open field lines extend from the central object and from the disc, and closed field lines connect the central object with the inner disc. However, there are several differences between the two cases.

(1) In L95 the central object is a neutron star, and the magnetic field lines are frozen at its surface. The open field lines are produced by the toroidal magnetic flux which is generated out of the closed field lines, arising from the difference of angular velocities between the neutron star and the disc. While the central object is a rotating BH in the BZ-MC-BP model, and the field lines can slip on the BH horizon. The coexistence of the open and the closed field lines at the BH horizon has been argued in W06. In the BZ-MC-BP model we assume that the open magnetic field at region II is amplified by the dynamo process, being brought inwards by the disc accretion, and the critical radii ( $r_{SIMC}$  and  $r_{SIBZ}$ ) provide a natural constraint to the open field lines extending from the disc to infinity as shown in Figure 1.

(2) The directions of the open field lines across the separatrix are opposite in L95, implying a current sheet exists along the separatrix. A magnetic reconnection might start from this configuration. In the BZ-MC-BP model, as shown in Figure 1, the open field lines in region I and II are in the same direction, which can be continuous across the separatrix, and the open magnetic field at region II is balanced by the magnetic pressure in the regions I and III.

(3) In L95 the magnetic field lines in region I penetrate the disc vertically, and an outflow cannot be driven centrifugally in the BP process. Contrary to L95, as shown in Figure 1, the poloidal magnetic field in region II could make an angle greater than  $30^\circ$  with the normal of the disc surface, and an outflow of matter driven centrifugally by the open magnetic field is permitted.

Following BP82, we assume that the poloidal magnetic field in region II varies with the disc radius  $r_d$  as follows,

$$(B_d^P)_{BP} \propto r_d^{-5/4}. \quad (3)$$

Considering the balance of the magnetic pressure across the boundary of region II and III, we have

$$(B_d^P)_{BP} = B_{MC} (r_d/r_{SIMC})^{-5/4} = B_{MC} (\xi/\xi_{SIMC})^{-5/4}, \quad (4)$$

where  $B_{MC}$  is the magnetic field at  $r_{SIMC}$ , and  $\xi \equiv r_d/r_{ms}$  is the disc radius in terms of  $r_{ms}$ .

According to W03 the magnetic field  $B_{MC}$  is related to the magnetic field at the horizon,  $B_H$ , by

$$B_H 2\pi (\varpi\rho)_{r=r_H} d\theta = -B_{MC} 2\pi (\varpi\rho/\sqrt{\Delta})_{\theta=\pi/2} dr_d. \quad (5)$$

where  $\varpi$ ,  $\rho$  and  $\Delta$  are the Kerr metric coefficients, and they read

$$\begin{cases} \varpi = (\Sigma/\rho) \sin \theta, \\ \Sigma^2 \equiv (r^2 + a^2)^2 - a^2 \Delta \sin^2 \theta, \\ \rho^2 \equiv r^2 + a^2 \cos^2 \theta, \\ \Delta \equiv r^2 + a^2 - 2Mr. \end{cases} \quad (6)$$

The angular coordinate  $\theta$  on the BH horizon is related

to the dimensionless disc radius  $\xi$  by the following mapping relation:

$$\cos \theta - \cos \theta_L = \int_1^\xi G(a_*, \xi, n) d\xi, \quad (7)$$

where the function  $G(a_*, \xi, n)$  has been given in W03 as follows,

$$G(a_*, \xi, n) = \frac{\xi^{1-n} \chi_{ms}^2 \sqrt{1+a_*^2 \chi_{ms}^{-4} \xi^{-2} + 2a_*^2 \chi_{ms}^{-6} \xi^{-3}}}{2\sqrt{(1+a_*^2 \chi_{ms}^{-4} + 2a_*^2 \chi_{ms}^{-6})(1-2\chi_{ms}^{-2} \xi^{-1} + a_*^2 \chi_{ms}^{-4} \xi^{-2})}}. \quad (8)$$

In equation (8)  $\chi_{ms}$  is defined in terms of the radius of the innermost stable circular orbit,  $r_{ms} = M\chi_{ms}^2$ , which is regarded as the inner edge of the disc. Incorporating equations (5) and (7), we have

$$B_{MC} = \frac{B_H}{\xi \chi_{ms}^4 \sqrt{1+a_*^2 \xi^{-2} \chi_{ms}^{-4} + 2a_*^2 \xi^{-3} \chi_{ms}^{-6}}} G(a_*, \xi, n) \Big|_{\xi=\xi_{SIMC}}. \quad (9)$$

where  $q \equiv \sqrt{1-a_*^2}$  is a function of the BH spin  $a_*$ . Thus we can determine the poloidal magnetic field in region II by combining equation (4) with equation (9).

### 3 OUTFLOW RATE, POWER AND TORQUE IN BP PROCESS

#### 3.1 Condition for outflow driven in hydromagnetic regime

As argued in BP82, an outflow of matter can be launched centrifugally, only if the angle of the poloidal component of the magnetic field with the normal of the disc is greater than a critical value, i.e.,  $\alpha_{FL} > 30^\circ$ . We can discuss the condition for driving the outflow based on the magnetic configurations given in Figure 1, and the angle  $\alpha_{FL}$  can be estimated by

$$\alpha_{FL} = \tan^{-1} [(\xi_{SIBZ} - \xi_{SIMC}) \chi_{ms}^2 / h_c], \quad (10)$$

where  $h_c \equiv H_c/M$  is the dimensionless height of the load above the disc surface.

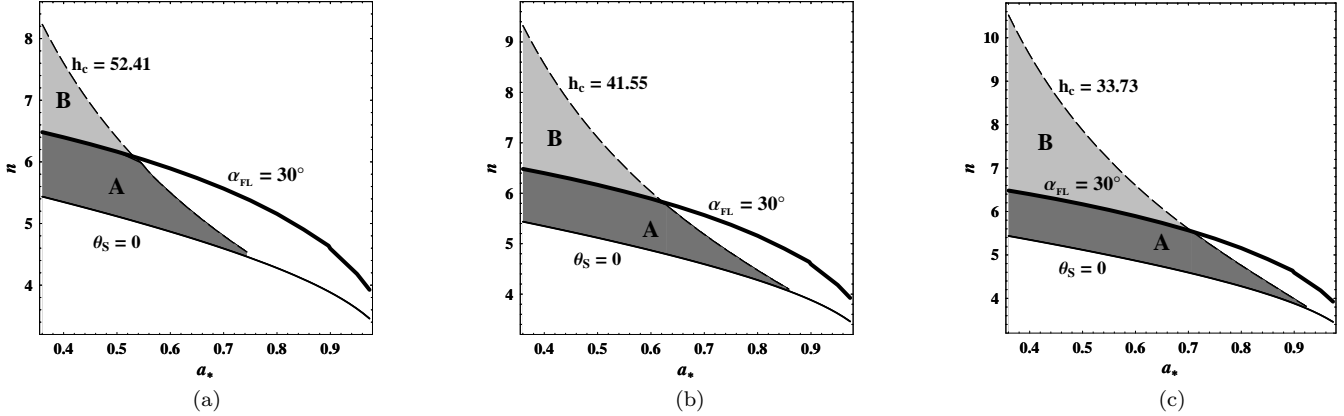
Incorporating equation (10) with the criteria (1) and (2), we obtain the values of  $\alpha_{FL}$  corresponding to the concerned parameters of SIBZ and SIMC as shown in Table 1, in which we have  $\alpha_{FL} > 30^\circ$  for driving the outflow in the hydromagnetic regime.

It is shown in Table 1 that the angle  $\alpha_{FL}$  can be determined by three parameters,  $a_*$ ,  $n$  and  $h_c$ , and the correlation of  $\alpha_{FL}$  with the three parameters is depicted in the  $a_* - n$  parameter space for the given  $h_c$  in Figure 2. The coexistence of SIBZ and SIMC is indicated by the shaded regions, which are bounded by two contours, i.e.,  $\theta_S = 0$  and  $h_c = 52.41, 41.55$  and  $33.73$  in Figure 2a, 2b and 2c, respectively. Each shaded region is further divided by the contour of  $\alpha_{FL} = 30^\circ$ , below and above which we have  $\alpha_{FL} < 30^\circ$  and  $\alpha_{FL} > 30^\circ$  in regions A and B, respectively.

Thus the two regimes of outflows driven can be determined by regions A and B, which correspond to the Poynting flux regime and hydromagnetic regime, respectively. In this paper we confine the discussion to the BP process by taking the values of  $a_*$  and  $n$  in region B.

**Table 1.** The angle  $\alpha_{FL}$  corresponding to the parameters of SIBZ and SIMC

$a_*$	$n$	$h_c$	$\xi_{SIBZ}$	$\xi_{SIMC}$	$\alpha_{FL}$
0.40	7.6	52.41	12.67	2.20	42.7 <sup>0</sup>
0.50	7.1	41.55	10.64	2.21	40.7 <sup>0</sup>
0.60	6.6	33.73	9.31	2.22	38.8 <sup>0</sup>
0.70	6.1	27.40	8.39	2.23	37.3 <sup>0</sup>
0.80	5.6	21.55	7.74	2.22	36.7 <sup>0</sup>

**Figure 2.** The shaded regions between the contour of  $\theta_S=0$  for (solid line) and the contours of  $h_c$ (dashed lines) are divided by the contour of  $\alpha_{FL}=30^\circ$  (thick solid line) for  $h_c = 52.41, 41.55$  and  $33.73$  in Figures 2a, 2b and 2c, respectively. Regions A and B indicate the parameters for  $\alpha_{FL}$  less and greater than  $30^\circ$ , respectively.

### 3.2 Rate of matter outflow and BP power and torque

Since angular momentum is transferred magnetically from a rotating BH to the inner disc in the MC process, the accretion rate is probably depressed. Thus we assume that the accretion rate in region II obeys the following relation,

$$\dot{M}_d/dr_d > 0, \quad \text{for} \quad r_{SIMC} < r_d < r_{out}. \quad (11)$$

Based on mass conservation the outflow rate is given by

$$\dot{M}_{outflow} = (\dot{M}_d)_{out} - (\dot{M}_d)_{MC}, \quad (12)$$

where  $(\dot{M}_d)_{MC}$  and  $(\dot{M}_d)_{out}$  are the accretion rates at  $r_{SIMC}$  and  $r_{out}$ , respectively.

As the magnetic field on the BH horizon is supported by the surrounding disc, there are some relations between  $B_H$  and  $\dot{M}_d$ . One of them is given by considering the balance between the magnetic pressure on the horizon and the ram pressure of the innermost parts of an accretion flow (Moderski, Sikora & Lasota 1997), i.e.,

$$B_H^2/(8\pi) = P_{ram} \sim \rho c^2 \sim \dot{M}_d/(4\pi r_H^2), \quad (13)$$

As a simple analysis, we take the accretion rate in region III as a constant, which is related to the magnetic field at BH horizon by the following relation,

$$(\dot{M}_d)_{MC} = \alpha_m B_H^2 r_H^2 \quad (14)$$

In equation (14) the parameter  $\alpha_m$  is an adjustable parameter due to the uncertainty of equation (13), and we take  $\alpha_m = 0.1$  in calculations.

Assuming that the accretion rate in region II varies with disc radius in a power-law,  $\dot{M}_d \propto r_d^S$ , we obtain its expression by combining equation (14) as follows,

$$\dot{M}_d = \alpha_m B_H^2 r_H^2 (r_d/r_{SIMC})^S \quad \text{for} \quad r_{SIMC} < r_d < r_{out} \quad (15)$$

or

$$\dot{m}_d \equiv \dot{M}_d/B_H^2 M^2 = \alpha_m (1+q)^2 (\xi/\xi_{SIMC})^S \quad \text{for} \quad \xi_{SIMC} < \xi < \xi_{out} \quad (16)$$

where  $B_H^2 M^2 \equiv (B_A^2 m_H^2 \times 7.32 \times 10^7) g \cdot s^{-1}$ .

Thus the outflow rate from a ring with width  $r_d - r_d + dr_d$  can be expressed as

$$d\dot{m}_{outflow} = \alpha_m (1+q)^2 S (\xi/\xi_{SIMC})^{S-1} d(\xi/\xi_{SIMC}), \quad (17)$$

and the total outflow rate driven from region II is

$$\dot{m}_{outflow} = \alpha_m (1+q)^2 (s_{out}^S - 1), \quad (18)$$

where  $\dot{m}_{outflow} \equiv \dot{M}_{outflow}/B_H^2 M^2$  and  $s_{out} \equiv \xi_{out}/\xi_{SIMC}$ .

According to BP82 the specific energy  $e$  and angular momentum  $l$  are constants along each open field line, and they read

$$e = v^2/2 + h + \Phi - \omega r B_\phi/k, \quad l = r v_\phi - r B_\phi/k. \quad (19)$$

The quantities involved in equation (19) are interpreted as follows. The quantity  $r$  is the cylindrical radius, and  $\omega$  is

the angular velocity of the foot point of the field line, being taken as Keplerian angular velocity of a thin disc and remaining constant along the field line. The quantities  $h$  and  $\Phi$  are respectively the enthalpy per unit mass and gravitational potential, and the quantities  $v$  and  $v_\varphi$  are the velocity of the streaming gas and its toroidal component, respectively. The parameter  $k$  is defined as

$$k/4\pi = \rho_m v_P / B_P, \quad (20)$$

which is interpreted as the ratio of the mass flux to the magnetic flux, and it also remains constant along each field line. The quantities  $\rho_m$  and  $v_P$  are the mass density and the poloidal velocity of the streaming gas, respectively. The toroidal velocity  $v_\varphi$  is related to the toroidal magnetic field  $B_\varphi$  by

$$v_\varphi = v_P B_\varphi / B_P + r\omega, \quad (21)$$

where  $v_P B_\varphi / B_P$  is the toroidal velocity of the streaming gas with respect to the rotating field line, and  $r\omega$  is the toroidal velocity of the field line itself. Incorporating equations (19)–(21), we have

$$B_\varphi = \frac{k(r\omega - l/r)}{1 - (v_P/v_{AP})^2} = \frac{k r \omega (1 - \lambda r_d^2/r^2)}{1 - (v_P/v_{AP})^2}, \quad (22)$$

where  $v_{AP} \equiv B_P / \sqrt{4\pi\rho}$  is the poloidal component of the Alfvén velocity, and  $\lambda \equiv l/r_d^2\omega$  is defined as the ratio of the specific angular momentum to that at the midplane of the disc in BP82.

Incorporating equations (19)–(22), we have

$$v_\varphi = r\omega \left[ 1 + \frac{(v_P/v_{AP})^2 (1 - \lambda r_d^2/r^2)}{1 - (v_P/v_{AP})^2} \right]. \quad (23)$$

According to BP82 the term  $-\omega r B_\varphi / k$  in equation (19) represents the work done on the streaming gas by the magnetic torque. Combining equation (22) with the work of the magnetic torque and the outflow rate, we derive the BP power and torque as follows,

$$\begin{aligned} dP_{BP} &= (-\omega r B_\varphi / k) d\dot{M}_{outflow} \\ &= \frac{\omega^2 (\lambda r_d^2 - r^2)}{1 - (v_P/v_{AP})^2} d\dot{M}_{outflow}, \end{aligned} \quad (24)$$

$$dT_{BP} = dP_{BP} / \omega = \frac{\omega (\lambda r_d^2 - r^2)}{1 - (v_P/v_{AP})^2} d\dot{M}_{outflow}. \quad (25)$$

In order to avoid the infinite BP power and torque at the Alfvén surface as  $v_P \rightarrow v_{AP}$ , we have

$$\lambda = (r_A/r_d)^2. \quad (26)$$

And equations (24) and (25) can be rewritten as

$$dP_{BP} = \frac{\omega^2 (r_A^2 - r^2)}{1 - (v_P/v_{AP})^2} d\dot{M}_{outflow}, \quad (27)$$

$$dT_{BP} = dP_{BP} / \omega = \frac{\omega (r_A^2 - r^2)}{1 - (v_P/v_{AP})^2} d\dot{M}_{outflow}. \quad (28)$$

Since the velocity of the gas increases with the cylinder radius in approaching the Alfvén velocity, we assume that  $v_P$  varies with  $r$  as follows,

$$v_P/v_{AP} = (r/r_A)^\alpha, \quad (29)$$

where  $\alpha$  is a parameter to be determined. Substituting equation (29) into equation (27) and taking limit for  $r \rightarrow r_A$  by using L'Hospital law, we have

$$dP_{BP} = \lim_{r \rightarrow r_A} \frac{\omega^2 (r_A^2 - r^2)}{1 - (r/r_A)^{2\alpha}} d\dot{M}_{outflow} = \frac{\omega^2 r_A^2}{\alpha} d\dot{M}_{outflow}. \quad (30)$$

Considering the fact that  $B_\varphi$  is dominative over  $B_P$  near the Alfvén surface, we infer that  $v_P \ll v_\varphi$  and take the specific kinetic energy of the streaming gas as  $\omega^2 r_A^2 / \alpha$  with  $\alpha = 2$  in equation (30). Substituting equation (26) into equation (30), we express the BP power and torque at the Alfvén surface as follows,

$$dP_{BP} = (\lambda/2) \omega^2 r_d^2 d\dot{M}_{outflow}, \quad (31)$$

$$dT_{BP} = (\lambda/2) \omega r_d^2 d\dot{M}_{outflow}. \quad (32)$$

Incorporating equation (17) and integrating equations (31) and (32) from  $\xi_{SIMC}$  to  $\xi_{out}$ , we have

$$\tilde{P}_{BP} = (\lambda \alpha_m / 2) \frac{(1+q)^2}{\xi_{SIMC} \chi_{ms}^2} \frac{S (\zeta_{out}^{S-1} - 1)}{S-1}, \quad (33)$$

$$\tilde{T}_{BP} = (\lambda \alpha_m / 2) (1+q)^2 \chi_{ms} \xi_{SIMC}^{1/2} \frac{S (\zeta_{out}^{S+1/2} - 1)}{S+1/2}, \quad (34)$$

where  $\tilde{P}_{BP} \equiv P_{BP}/P_0$ ,  $\tilde{T}_{BP} \equiv T_{BP}/T_0$  and

$$\begin{cases} P_0 \equiv \langle B_H^p \rangle^2 M^2 \approx B_4^2 m_H^2 \times 6.59 \times 10^{28} \text{ erg} \cdot \text{s}^{-1} \\ T_0 \equiv \langle B_H^p \rangle M^3 \approx B_4^2 m_H^3 \times 3.26 \times 10^{23} \text{ g} \cdot \text{cm}^2 \cdot \text{s}^{-2} \end{cases} \quad (35)$$

The powers and torques in the BZ and MC processes have been derived in W02 as follows,

$$\tilde{P}_{BZ} \equiv P_{BZ}/P_0 = 2a_*^2 \int_0^{\theta_S} \frac{k(1-k) \sin^3 \theta d\theta}{2 - (1-q) \sin^2 \theta}, \quad (36)$$

$$\tilde{T}_{BZ} \equiv T_{BZ}/T_0 = 4a_* (1+q) \int_0^{\theta_S} \frac{(1-k) \sin^3 \theta d\theta}{2 - (1-q) \sin^2 \theta}, \quad (37)$$

$$\tilde{P}_{MC} \equiv P_{MC}/P_0 = 2a_*^2 \int_{\theta_S}^{\theta_L} \frac{\beta(1-\beta) \sin^3 \theta d\theta}{2 - (1-q) \sin^2 \theta}, \quad (38)$$

$$\tilde{T}_{MC} \equiv T_{MC}/T_0 = 4a_* (1+q) \int_{\theta_S}^{\theta_L} \frac{(1-\beta) \sin^3 \theta d\theta}{2 - (1-q) \sin^2 \theta}, \quad (39)$$

where  $k$  and  $\beta$  are the ratios of the angular velocity of the field line to that of the BH horizon in the BZ and MC processes, respectively.

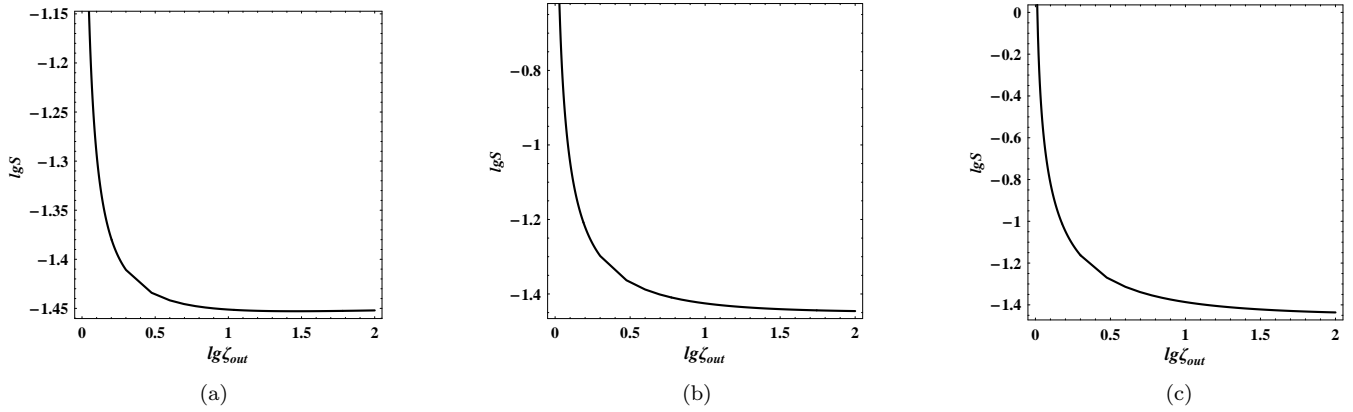
Now we are going to discuss the relation between the power-law index  $S$  and the ratio  $\zeta_{out}$  based on the transfer of angular momentum from region III to region II.

It is assumed that the accretion rate  $(\dot{M}_d)_{out}$  at  $r_{out}$  is related to  $(\dot{M}_d)_{MC}$  by

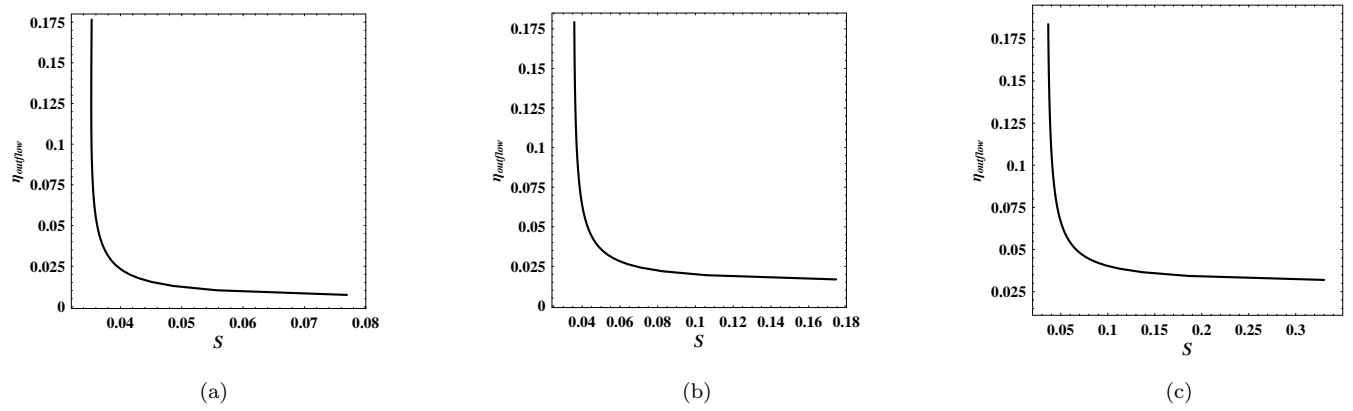
$$(\dot{M}_d)_{out} (r^2 \omega)_{out} - (\dot{M}_d)_{MC} (r^2 \omega)_{SIMC} = T_{BP} - \delta T_{MC}, \quad (40)$$

where  $\delta T_{MC} = T_{MC}^{in} - T_{MC}^{out}$  is the angular momentum transferred from region III to region II, and  $\delta$  is a fraction parameter taken as  $\delta = 0.5$  in calculations. The terms  $T_{MC}^{in}$  and  $T_{MC}^{out}$  are the transfer rates of angular momentum at  $r_{SIMC}$  and  $r_{out}$ , respectively. Substituting equation (15) into equation (40), we have

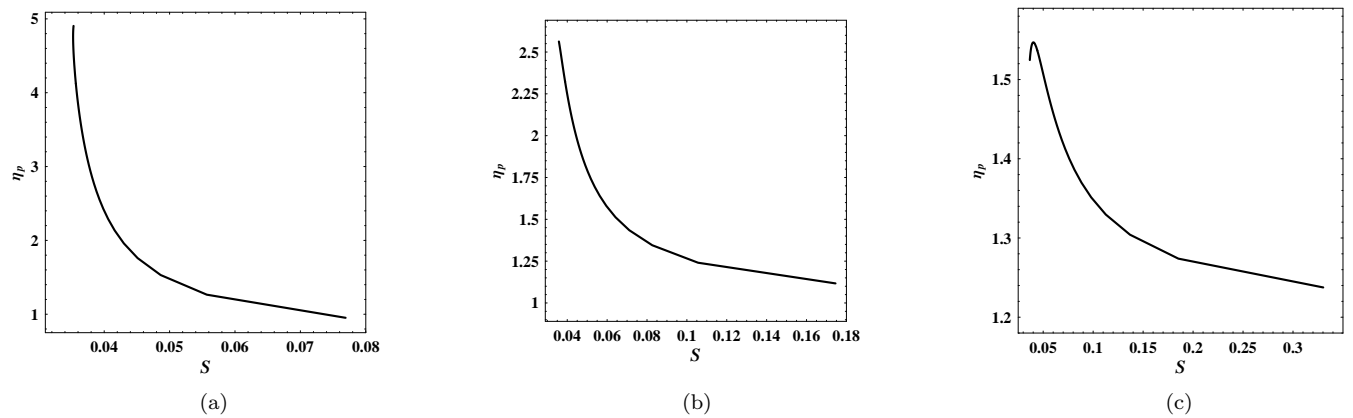
$$\alpha_m B_H^2 r_H^2 [\zeta_{out}^S (r^2 \omega)_{out} - (r^2 \omega)_{MC}] = T_{BP} - \delta T_{MC}. \quad (41)$$



**Figure 3.** The curves of  $lgS$  versus  $lgz_{out}$  for different values of  $a_*$  and  $n$ , (a)  $a_* = 0.40$ ,  $n = 7.6$  (b)  $a_* = 0.60$ ,  $n = 6.6$  and (c)  $a_* = 0.80$ ,  $n = 5.6$ .



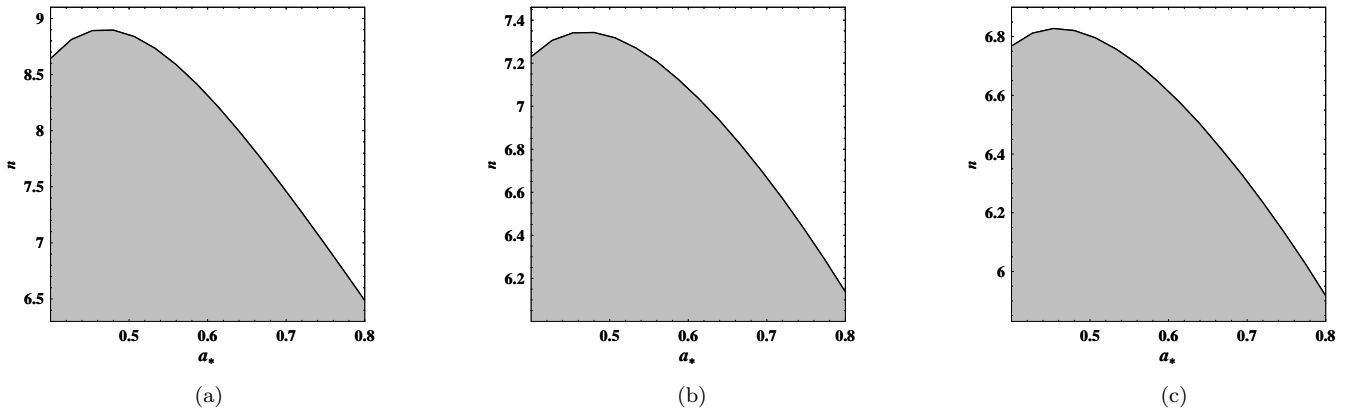
**Figure 4.** The curves of  $\eta_{outflow}$  versus  $S$  for different values of  $a_*$  and  $n$ , (a)  $a_* = 0.40$ ,  $n = 7.6$  (b)  $a_* = 0.60$ ,  $n = 6.6$  and (c)  $a_* = 0.80$ ,  $n = 5.6$ .



**Figure 5.** The curves of  $\eta_p$  versus  $S$  for different values of  $a_*$  and  $n$ , (a)  $a_* = 0.40$ ,  $n = 7.6$  (b)  $a_* = 0.60$ ,  $n = 6.6$  and (c)  $a_* = 0.80$ ,  $n = 5.6$ .

**Table 2.** The values of the derived parameters with  $\xi_{out}/\xi_{SIMC} = 10^2$ 

$a_*$	$n$	$h_c$	$\xi_{SIBZ}$	$\xi_{SIMC}$	$S$
0.40	7.6	52.41	12.67	2.20	0.0353
0.50	7.1	41.55	10.64	2.21	0.0355
0.60	6.6	33.73	9.31	2.22	0.0358
0.70	6.1	27.40	8.39	2.23	0.0362
0.80	5.6	21.55	7.74	2.22	0.0366


**Figure 6.** The inequality  $\tilde{P}_{BP} > \tilde{P}_{BZ}$  with  $\eta_P > 1$  holds in the shaded region for (a)  $S = 0.2$ , (b)  $S = 0.4$  and (c)  $S = 0.6$ .

Equation (41) can be rewritten as

$$\alpha_m (1+q)^2 \chi_{ms} \varsigma_{out}^S \left( \xi_{out}^{1/2} - \xi_{SIMC}^{1/2} \right) = \tilde{T}_{BP} - \delta \tilde{T}_{MC}. \quad (42)$$

Equations (33)–(42) provide a closed set for calculating the powers and torques in the BZ, MC and BP processes, in which seven parameters are  $a_*$ ,  $n$ ,  $h_c$ ,  $\alpha_m$ ,  $\delta$ ,  $S$  and  $\varsigma_{out}$  are involved. Besides the parameters  $\alpha_m = 0.1$  and  $\delta = 0.5$  the rest five parameters are divided into two types.

(1) The parameters  $a_*$ ,  $n$  and  $h_c$  are required to be greater than some critical values for the coexistence of SIBZ and SIMC as argued in W06, by which the boundary radii  $\xi_{SIMC}$  and  $\xi_{SIBZ}$  can be determined.

(2) The parameters  $S$  and  $\varsigma_{out}$  are involved in the BP process, and only one of them is independent as shown in Figure 3 below.

Thus we have four independent parameters ( $a_*$ ,  $n$ ,  $h_c$  and  $\varsigma_{out}$ ) as the input parameters, and  $\xi_{SIMC}$ ,  $\xi_{SIBZ}$  and  $S$  as the derived parameters. Based on the above analysis we have the values of the derived parameters corresponding to the input ones as listed in Table 2.

Based on equations (34), (39) and (42) we obtain the curves of the parameter  $S$  varying with  $\varsigma_{out}$  for the given values of  $a_*$  and  $n$  as shown in Figure 3, and we find that  $S$  decreases monotonically with the increasing  $\varsigma_{out}$ .

Incorporating equations (16) and (18), we have the ratio of  $\dot{M}_{outflow}$  to  $\dot{M}_d$  expressed by

$$\eta_{outflow} = \dot{M}_{outflow} / (\dot{M}_d)_{MC} = \varsigma_{out}^S - 1, \quad (43)$$

and the curves of  $\eta_{outflow}$  versus  $S$  for the given values of  $a_*$  and  $n$  are shown in Figure 4.

Inspecting Figure 4, we find that  $\eta_{outflow}$  decreases monotonically with the increasing  $S$ , and this result implies that the greater ratio  $\varsigma_{out}$  corresponds to the less  $S$  and the greater outflow rate.

#### 4 JET POWER FROM BH ACCRETION DISCS

As argued above the jets are driven respectively in the Poynting flux and hydromagnetic regimes by the BZ and BP processes, and the jet power can be estimated as the sum of the BZ and BP powers,

$$P_{jet} = P_{BZ} + P_{BP}. \quad (44)$$

Thus we have the powers and torques in the BZ-MC-BP model as shown in Table 3.

The results listed in Table 3 correspond to  $\varsigma_{out} = 10^2$ , and we find that the BP power is greater than the BZ power, while the BP torque is about two orders greater than the BZ torque. Based on equations (33)–(39) we have the curves of  $\eta_P \equiv P_{BP}/P_{BZ}$  versus  $S$  for the given values of  $a_*$  and  $n$  as shown in Figure 5.

Inspecting Figure 5, we find that the ratio  $\eta_P > 1$  holds for a variety of values of the parameters,  $a_*$ ,  $n$  and  $S$ . Combining Figure 5 with Figure 3, we find that the BP power can be more stronger than the BZ power for less  $S$  and thus for greater  $\varsigma_{out}$ .

In order to discuss the relative importance of the BP power relative to the BZ power in a visual way we plot the contour of  $\eta_P = 1$  in  $a_* - n$  parameter space for the given

**Table 3.** The powers and torques in the BZ, MC and BP model with  $s_{out} = 10^2$ 

$a_*$	$n$	$h_c$	$\tilde{T}_{BZ}$	$\tilde{T}_{BP}$	$\tilde{P}_{BZ} (\times 10^{-3})$	$\tilde{P}_{BP} (\times 10^{-3})$	$\tilde{P}_{jet} (\times 10^{-3})$
0.40	7.6	52.41	0.077	12.57	4.00	19.73	23.73
0.50	7.1	41.55	0.089	11.42	5.94	20.36	26.30
0.60	6.6	33.73	0.098	10.14	8.18	20.81	28.99
0.70	6.1	27.40	0.107	8.68	10.89	21.18	32.07
0.80	5.6	21.55	0.118	6.97	14.69	21.71	36.40

values of  $\mathcal{S}$  as shown in Figure 6, in which the shaded regions indicate  $\eta_P > 1$  for the BP power greater than the BZ power.

Incorporating Figures 5 and 6, we find that the BP power could be greater than the BZ power for a wide range of the parameters  $a_*$ ,  $n$  and  $\mathcal{S}$ . These results are consistent with the previous works in estimating the BZ power relative to the jet power from the inner disc (Ghosh & Abramowicz 1997; Livio, Ogilvie & Pringle 1999).

Cao & Rawlings (2004, hereafter CR04) estimated the jet powers of a sample of 3CR FR I radio galaxies, and they argued that the BZ mechanism provides insufficient power to explain the high radio luminosities of at least a third, and perhaps all, of the sample, if the accretion discs in these sources are assumed to be advection dominated accretion flows (ADAFs), or adiabatic inflow-outflow solution (ADIOS) flows. However, the BP power was not considered in CR04. From Table 3 we find that  $P_{jet} = (2.5 \sim 6) P_{BZ}$ , and the jet powers can be amplified significantly by using equation (44).

## 5 DISCUSSION

In this paper we incorporate three mechanisms into the BZ-MC-BP model, in which the jet can be powered by both BZ and BP mechanisms, which belong to the Poynting flux and the hydromagnetic regimes, respectively. In this model the ratio of the BP power to the BZ power varies with the concerned parameters,  $a_*$ ,  $n$  and  $\mathcal{S}$ , as shown in Table 3 and Figure 5.

As pointed out by Meier (2003), there are observational reasons for believing that the same source may produce jets of rather different Lorentz factors, either simultaneously or in different accretion states. The results obtained in this model could interpret the jets of different Lorentz factors, and are consistent with a spine/sheath jet structure. The Poynting flux powered by the BZ process corresponds to the spine with higher Lorentz factor near the axis and hydromagnetic outflow powered by the BP process corresponds to the sheath with lower Lorentz factor away from the axis.

Another feature of this model is the role of the MC process. It is assumed that disc accretion is depressed due to the transfer of the angular momentum from a rotating BH to the inner disc. It is the MC effects that give rise to the variation of the accretion rate as well as the outflow in region II. It has been argued that a very steep emissivity index required by broad Fe K $\alpha$  lines can be interpreted by invoking the MC process, which is consistent with the *XMM-*

*Newton* observation of the nearby bright Seyfert 1 galaxy MCG-6-30-15 (Wilms 2001; Li 2002c; W03).

Recently, Sambruna et al. (2006) discussed the jet/accretion connection based on Chandra and XMM-Newton observations of three powerful radio-loud quasars, 1136-135, 1150+497 (*Chandra*), and 0723+679 (*XMM-Newton*), and they concluded that both jet and disc emission contribute to the X-ray emission from the three quasar cores. It was pointed out that the beamed emission contributes roughly 50% to the total flux in 2-10 keV, while the disc emission dominates below 2 keV. We expect that the jet/accretion connection in these radio-loud quasars could be interpreted based on the BZ-MC-BP model, in which the jet power is equal to the sum of the BZ and BP powers, and the MC power plus the disc accretion power can be used to fit the disc luminosity. In addition, the different Lorentz factor in the jet can be fitted by adjusting the ratio of the BP power to the BZ power, and the broad Fe K $\alpha$  lines can be simulated by invoking the MC process as argued in W03.

Very recently, Wang, Ye & Huang, (2007, hereafter W07) fitted the twin peak high frequency quasi-periodic oscillations (QPOs) associated with the jets observed in several sources, in which BH binary GRO J1655-40 is included. The fitting in W07 is focused on the association of the 3:2 QPO pairs of the jets based on the coexistence of the BZ and MC mechanisms, in which the jet is powered by the BZ process and the MC process is invoked to fit the 3:2 QPO pairs. It is noted that an X-ray-absorbing wind discovered in an observation of GRO J1655-40 must be powered by a magnetic process. Detailed spectral analysis and modeling of the wind shows that it can only be powered by pressure generated by magnetic viscosity internal to the disk or magnetocentrifugal forces (Miller et al. 2006). Thus we expect that the fitting given in W07 should be improved based on the BZ-MC-BP model.

Recently, a lot of works have been done on general relativistic simulation on BH accretion and outflow (De Villiers, Hawley & Krolik 2003; Hirose, Krolik, De Villiers & Hawley 2004; De Villiers, Hawley, Krolik & Hirose 2005; Krolik, Hawley, & Hirose 2005). McKinney & Narayan (2007) have found that a highly relativistic, Poynting-dominated funnel jet in the polar regions of a Kerr BH is associated with a strikingly simple angular-integrated toroidal current distribution  $dI_\varphi/dr \propto r^{-3/4}$ , and the polar field is confined/collimated by the corona. It is interesting to note that the BZ-MC-BP model is consistent with the simulations in some main features: (1) Poynting-dominated jets driven by the BZ process, and (2) a large-scale poloidal magnetic field varying with the disc radius as  $B_d^p \propto r_d^{-n}$  corresponds to a



simple toroidal current with a power-law distribution in the disc. We shall improve this model based on the constraints of the numerical simulations as well as the observations in our future work.

## ACKNOWLEDGEMENTS

This work is supported by the National Natural Science Foundation of China under grants 10573006, 10703002 and 10121503. The anonymous referee is thanked for his/her helpful comments.

## REFERENCES

- Balbus S. A., Hawley J. F., 1998, *Rev. Mod. Phys.* 70, 1
- Bateman G., *MHD Instabilities*, 1978, (Cambridge: The MIT Press)
- Blandford R. D., Znajek R. L., 1977, *MNRAS*, 179, 433
- Blandford R. D., Payne, D. G., 1982, *MNRAS*, 199, 883 (BP82)
- Blandford R. D., 1999, in ASP Conf. Ser. 160, *Astrophysical Discs: An EC Summer School*, ed. J. A. Sellwood & J. Goodman (San Francisco: ASP), 265
- Cao X. W., Rawlings S., 2004, *MNRAS*, 349, 1419 (CR04)
- De Villiers J.-P., Hawley J. P., Krolik J. F., 2003, *ApJ*, 599, 1238
- De Villiers J.-P., Hawley J. P., Krolik J. F., Hirose S., 2005, *ApJ*, 620, 878
- Ghosh P., Abramowicz M. A. 1997, *MNRAS*, 292, 887
- Hirose S., Krolik J. F., De Villiers J.-P., Hawley J. P., 2004, *ApJ*, 606, 1083
- Kadomtsev B. B., 1966, *Rev. Plasma Phys.*, 2, 153
- Krolik J. F., Hawley J. P., Hirose S., 2005, *ApJ*, 622, 1008
- Li L.-X., 2000, *ApJ*, 533, L115
- . 2002a, *ApJ*, 567, 463
- Li L.-X., 2002b, *Phys. Rev. D*, 65 084047
- Li L.-X. 2002c, *A&A*, 392, 469
- Livio M., Ogilvie G. I., Pringle J. E., 1999, *ApJ*, 512, 100
- Lovelace R. V. E., Romanova M. M., Bisnovatyi-Kogan G. S., 1995, *MNRAS*, 275, 244 (L95)
- Lovelace R. V. E., Koldoba A. V., Ustyugova G. V., Romanova M. M., 2002, *ApJ*, 572, 445
- MacDonald D., Thorne K. S., 1982, *MNRAS*, 198, 345
- McKinney J. C., Narayan R., 2007, *MNRAS*, 375, 513
- Meier D. L., *New Astron. Rev.* 2003, 47, 667
- Miller J. M., Raymond J., Fabian A., Steeghs D., Homan J. Reynolds C., van der Klis M., Wijnands R., 2006, *Nature*, 441, 953
- Moderski R., Sikora M., Lasota J. P., 1997, in *Relativistic Jets in AGNs* eds.M. Ostrowski, M. Sikora, G. Madejski & M. Belgelman, Krakow, p.110
- Sambruna R. M., Gliozzi M., Tavecchio F., Maraschi L., Foschini L., 2006, *ApJ*, 652, 146
- Ustyugova G. V., Lovelace R. V. E., Romanova M. M., Li H., Colgate S. A., 2000, *ApJ*, 541, L21
- Uzdensky D. A., 2004, *ApJ*, 603, 652
- Uzdensky D. A., 2005, *ApJ*, 620, 889
- Wang D.-X., Xiao K., Lei W.-H., 2002, *MNRAS*, 335, 655 (W02)
- Wang D.-X., Ma R.-Y., Lei, W.-H., Yao, G.-Z., *ApJ*, 2003, 595, 109 (W03)
- Wang, D.-X., Lei, W.-H., Ye, Y.-C., 2006, *ApJ*, 643, 1047 (W06)
- Wang D.-X., Ye Y.-C., Li Y, Liu D.-M., *MNRAS*, 2007, 374, 647
- Wang D.-X., Ye Y.-C., Huang C.-Y., 2007, *ApJ*, 657, 428 (W07)
- Wilms J., Reynolds C. S., Begelman M. C., Reeves J., Molendi, S., Staubert R., Kendziorra E., 2001, *MNRAS*, 328, L27